



# CHORUS

This is the accepted manuscript made available via CHORUS. The article has been published as:

## Three-Dimensional Dynamic Localization of Light from a Time-Dependent Effective Gauge Field for Photons

Luqi Yuan and Shanhui Fan

Phys. Rev. Lett. **114**, 243901 — Published 16 June 2015

DOI: [10.1103/PhysRevLett.114.243901](https://doi.org/10.1103/PhysRevLett.114.243901)

# Three dimensional dynamic localization of light from a time-dependent effective gauge field for photons

Luqi Yuan and Shanhui Fan

*Department of Electrical Engineering, and Ginzton Laboratory,  
Stanford University, Stanford, CA 94305, USA*

(Dated: May 27, 2015)

## Abstract

We introduce a method to achieve three-dimensional dynamic localization of light. We consider a dynamically-modulated resonator lattice that has been previously shown to exhibit an effective gauge potential for photons. When such an effective gauge potential varies sinusoidally in time, dynamic localization of light can be achieved. Moreover, while previous works on such effective gauge potential for photons were carried out in the regime where the rotating wave approximation is valid, the effect of dynamic localization persists even when the counter-rotating term is taken into count.

PACS numbers: 42.60.Da, 63.20.Pw, 41.20.Jb

The effect of dynamic localization is of fundamental importance in understanding coherent dynamics of a charged particle in a periodic potential. When such a charged particle is in addition subjected to a time-harmonic external electric field, the wavefunction of the particle can become completely localized [1, 2]. This effect has been studied in a number of systems [3–13], and has been demonstrated in experiments involving Bose-Einstein condensate or optical lattices [14, 15].

Localization of photon, especially in full three dimensions, is of great practical and fundamental importance for the control of light [16, 17]. Anderson localization [18] of light, which uses disordered but time-independent photonic structures, have been extensively explored [19–21]. Dynamic localization of light, which uses ordered but time-dependent structures, provides a significant alternative. Photon is a neutral particle, thus there is no naturally occurring time-harmonic electric field that couples to photon. To achieve dynamic localization of photon, one therefore needs to synthesize an effective electric field. Up to now, extensive experimental and theoretical works has focused on light propagation in a waveguide array, where the effect of dynamic localization manifests by analogy as the cancellation of diffraction when the array is modulated in space along the propagation direction [22–27]. There has not been however any demonstration of a true three-dimensional localization of light in a photonic structure undergoing time-dependent modulation.

In this letter, we show that the concept of photonic gauge potential provides a mechanism to achieve dynamic localization of light in full three dimensions. It has been theoretically proposed [28] and experimentally demonstrated [29–31] that when the refractive index of a photonic structure is modulated in time sinusoidally, the phase of the modulation corresponds to an effective gauge potential for photon states [32–35]. Ref. [28–35] utilized this correspondence to create a spatially inhomogeneous, but time-invariant gauge potential distribution, in order to study effects associated with an effective magnetic field for photons, including the photonic Aharnov-Bohm effect [28, 29, 31], and the photonic analogue of the integer quantum hall effect [32]. In contrast, here we create a gauge potential that is spatially homogenous or periodic, but temporally varying. We show that such a time-dependent gauge potential naturally leads to a time-varying effective electric field for photons, which can be used to create three-dimensional dynamic localization of light. Moreover, while Ref. [28, 32–35] have only considered the regime where the rotating wave approximation is valid, here we show that such dynamic localization persist even when the counter-rotating term is

taken into account.

We start with the same model system as discussed in details in Refs. [32, 33], consisting of either a one-dimensional or three-dimensional photonic resonator lattice as shown in Fig. 1. The lattice consists of two types of resonators ( $A$  and  $B$ ) with frequencies  $\omega_A$  and  $\omega_B$  respectively. The Hamiltonian of the system is

$$H = \omega_A \sum_m a_m^\dagger a_m + \omega_B \sum_n b_n^\dagger b_n + \sum_{\langle mn \rangle} V \cos(\Omega t + \phi_{mn}(t))(a_m^\dagger b_n + b_n^\dagger a_m), \quad (1)$$

where  $V \cos(\Omega t + \phi_{mn}(t))$  is the coupling strength between the nearest neighbor resonators.  $\Omega = \omega_A - \omega_B$ .  $\phi_{mn}$  is the phase of the coupling strength modulation. In this paper, we will consider the situations where such modulation phase itself is modulated in time, and refer to such modulation of the phase  $\phi_{mn}$  as the *phase modulation*.  $a^\dagger$  ( $a$ ) and  $b^\dagger$  ( $b$ ) are the creation (annihilation) operators in the  $A$  and  $B$  sublattice, respectively.

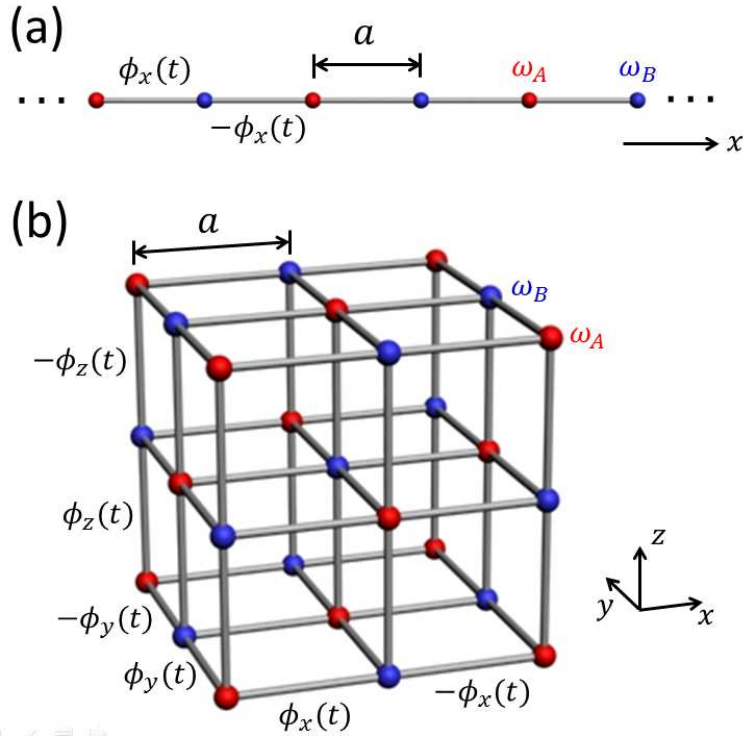


FIG. 1: (color online) A one-dimensional (a) and a three-dimensional (b) photonic resonator lattice where two kinds of resonators with frequency  $\omega_A$  (red dots) and  $\omega_B$  (blue dots). The nearest-neighbor coupling is dynamically modulated and the phase of the coupling constant modulation itself can be time-dependent with the signs being flipped between two neighboring bonds. The lattice is assumed infinite in all directions.

We note that Eq. (1) can be derived from Maxwell's equations in three dimensions. The derivation is provided in the Supplementary Information [36]. The key point here is that one can construct a vectorial modal basis upon which the three-dimensional electromagnetic fields can be expanded. The dynamics of the modal expansion coefficients can then be described in the form that is reminiscent of the schr odinger equation with a tight-binding Hamiltonian, which forms the starting point of our investigation. This technique has been previously used in the literature to account for three-dimensional FDTD numerical simulations [37, 41–43] and actual experiments [44].

In the limit  $V \ll \Omega$ , the rotating wave approximation (RWA) is valid. Therefore, we can simplify the Hamiltonian and rewrite it in the rotating frame [32]

$$H = \sum_{\langle mn \rangle} \frac{V}{2} (e^{-i\phi_{mn}(t)} c_m^\dagger c_n + e^{i\phi_{mn}(t)} c_n^\dagger c_m), \quad (2)$$

where  $c_{m(n)} = e^{i\omega_{A(B)}t} a_m (b_n)$ . In general such a system has a dynamic effective gauge field [32]

$$\vec{A}_{mn}^{\text{eff}} = \hat{l}_{mn} \phi_{mn}(t)/a, \quad (3)$$

where  $\hat{l}_{mn}$  is a unit vector and  $a$  is the distance between two near-neighbor sites. Here however, we choose the modulation phases such that in Eq. (2), all bonds along the same direction have the same phase. e.g. all bonds along the  $x$ -direction has the same phase  $\phi_x(t)$ . In the three-dimensional case,  $\phi_y(t)$  and  $\phi_z(t)$  are similarly defined. Since the phases are uniform in space, the system has zero effective magnetic field.

We now show that with a proper choice of the time-dependency of these phases, we can achieve dynamic localization. As an illustration we consider the one-dimensional case in some details. The three-dimensional case naturally follows. In the one-dimensional case, as an intuitive analysis, we can write the Hamiltonian (2) in the wavevector space ( $\mathbf{k}$ -space)

$$H = \sum_{k_x} V c_{k_x}^\dagger c_{k_x} \cos[k_x a - \phi_x(t)]. \quad (4)$$

Hence the system has an instantaneous photonic band structure  $\omega(k_x) = V \cos[k_x a - \phi_x(t)] = V \cos[(k_x - A_x)a]$ . The effect of a spatially uniform photonic gauge potential is a shift of the bandstructure in  $\mathbf{k}$ -space ([33, 35]). Since the structure maintains translational invariance, the wavevector  $k_x$  is a conserved quantity throughout the modulation process. The group

velocity of the wave packet of the photon with wavevector  $k_x$  is given by

$$v_g(k_x) = \frac{\partial\omega(k_x)}{\partial k_x} = -Va \sin[k_x a - \phi_x(t)]. \quad (5)$$

At different values of  $\phi_x$ , the group velocity at the same wavevector can have either positive or negative signs.

To demonstrate dynamic localization, we choose a phase modulation of the form  $\phi_x(t) = \alpha_x \cos(\omega_M t)$ , where  $\alpha_x$  and  $\omega_M$  are the amplitude and the frequency of the phase modulation, respectively. Thus, the average group velocity over one phase modulation period  $2\pi/\omega_M$  is

$$\langle v_g(k_x) \rangle = -Va \sin(k_x a) J_0(\alpha_x), \quad (6)$$

where  $J_0$  is the zeroth-order Bessel function. by choosing  $\alpha_x$  be to a zero of  $J_0$ , (we denote one of such zero as  $\alpha$  below), the average group velocity is zero for all  $k_x$ . Thus all wavepackets of the system become localized, signifying the presence of dynamic localization. Importantly, the condition for dynamic localization here is related to the strength of the phase modulation, and independent of the phase modulation frequency  $\omega_M$ .

We confirm the intuitive analysis above based on the instantaneous bandstructure, by a rigorous numerical calculation of the Floquet eigenstates of Hamiltonian in Eq. (1). In this numerical analysis, we use the Hamiltonian of Eq. (4), and directly compute the quasi-energy  $\varepsilon$  at each  $k_x$ , following the same procedure as in Ref. [2, 45, 46]. The resulting  $\varepsilon$  as a function of phase modulation strength  $\alpha$ , for different  $k_x$ 's, are plotted in Figure 2. At each  $\alpha$ , the range of the values of the quasi-energy indicates the bandwidth of the quasi-energy bandstructure. The onset of the dynamic localization corresponds to the collapse of the bandwidth. In Figure 2, we indeed observe the collapse of bandwidth when the phase modulation strength approaches each of the zero's of  $J_0$ .

For the study of electronic dynamic localization, the effect of a time-varying electric field is typically described through the use of a spatially non-uniform *scalar* potential, as described by a Hamiltonian [1, 2]

$$\tilde{H} = \sum_{\langle mn \rangle} \frac{V}{2} (c_m^\dagger c_n + c_n^\dagger c_m) - \sum_n n \alpha \omega_M \sin(\omega_M t) c_n^\dagger c_n, \quad (7)$$

In contrast, we have used a *vector* potential that is spatially periodic. Our Hamiltonian of Eq. (2) is in fact equivalent to (Eq. (7)) by a gauge transformation:

$$|\Psi\rangle = \sum_n v_n c_n^\dagger |0\rangle \rightarrow |\tilde{\Psi}\rangle = \sum_n \tilde{v}_n c_n^\dagger |0\rangle = \sum_n v_n e^{i\theta_n} c_n^\dagger |0\rangle, \quad (8)$$

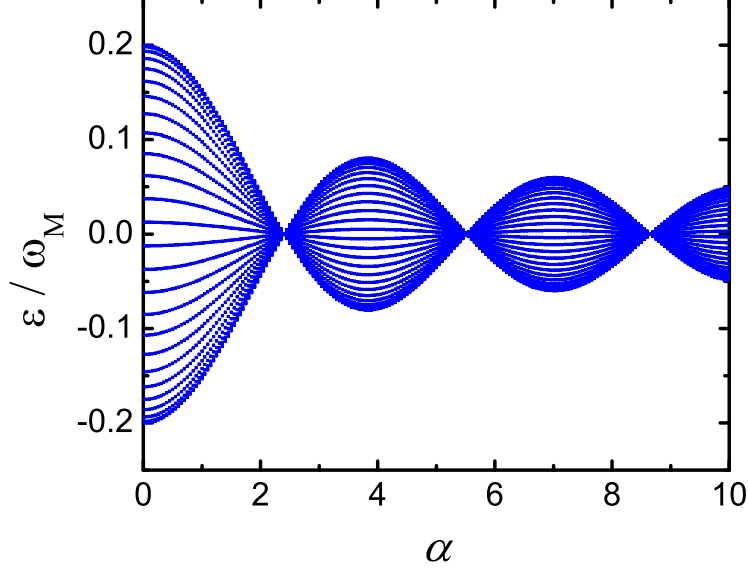


FIG. 2: (color online) The quasienergies as a function of  $\alpha$ , for the Hamiltonian of Eq. (4), with  $\phi_x(t) = \alpha \cos(\omega_M t)$ . Here we choose  $V = 0.2\omega_M$ . Each curve corresponds to a different wavevector  $k_x$ , in the range  $-\pi/a < k_x < \pi/a$ .

where  $|\Psi\rangle$  satisfies the Schrödinger equation  $i\frac{\partial}{\partial t}|\Psi\rangle = H|\Psi\rangle$  or  $i\dot{v}_n = \frac{V}{2} [e^{-i\alpha \cos(\omega_M t)} v_{n+1} + e^{i\alpha \cos(\omega_M t)} v_{n-1}]$ . With a gauge choice of  $\theta_n = -n\alpha \cos(\omega_M t)$ , the gauge-transformed state  $|\tilde{\Psi}\rangle$  then satisfies

$$\begin{aligned}
i\frac{\partial}{\partial t}|\tilde{\Psi}\rangle &= \sum_n i\dot{v}_n e^{i\theta_n} c_n^\dagger |0\rangle - \sum_n v_n \dot{\theta}_n e^{i\theta_n} c_n^\dagger |0\rangle \\
&= \frac{V}{2} \sum_n [e^{-i\alpha \cos(\omega_M t)} v_{n+1} + e^{i\alpha \cos(\omega_M t)} v_{n-1}] e^{i\theta_n} c_n^\dagger |0\rangle - \sum_n v_n \dot{\theta}_n e^{i\theta_n} c_n^\dagger |0\rangle \\
&= \frac{V}{2} \sum_n [v_{n+1} e^{i\theta_{n+1}} + v_{n-1} e^{i\theta_{n-1}}] c_n^\dagger |0\rangle - \sum_n n\alpha\omega_M \sin(\omega_M t) v_n e^{i\theta_n} c_n^\dagger |0\rangle \\
&= \tilde{H}|\tilde{\Psi}\rangle,
\end{aligned} \tag{9}$$

where  $\tilde{H}$  is given in Eq. (7). Therefore, the two Hamiltonians of Eqs. (2) and (7) are indeed equivalent to each other, as they are related by a gauge transformation. Similar gauge transformation has been used in the study of waveguide array [22]. Certainly, a time-varying gauge potential for an electron is related to an electric field applied on the electron. Here we have shown that a time-varying effective gauge potential for a photon also analogously produces an effective electric field applied on the photon.

Unlike the waveguide array approach, where the effect of photonic dynamic localization

manifests through an analogy as the cancellation of diffraction in a static structure, in our approach here one can directly achieve dynamic photon localization in all three dimensions. We consider the Hamiltonian of Eq. (1) for the three-dimensional lattice as shown in Figure 1(b). We choose the phase modulation  $\phi_{x,y,z}(t) = \alpha \cos(\omega_M t)$ . The intuitive derivation of dynamic localization condition (Eqs. (5)-(6)) can then be straightforwardly generalized to full three-dimension. Full three-dimensional dynamic localization is achieved provided that the modulation strength above is chosen to be a zero of the  $J_0$ , for all choices of phase modulation frequency  $\omega_M$ .

Similar to the one-dimensional case, the intuitive derivations for dynamic localization for three-dimension can be confirmed by a rigorous Floquet analysis showing band collapse. Instead, here we provide the evidence of full three-dimensional dynamic localization, by a direct simulation of photon dynamics in a  $40a \times 40a \times 40a$  three dimensional lattice. The simulation is done by solving the coupled-mode equation [34]

$$id|\Psi(t)\rangle/dt = H(t)|\Psi(t)\rangle. \quad (10)$$

Here  $|\Psi\rangle = [\sum_m v_m(t)a_m^\dagger + \sum_n v_n(t)b_n^\dagger] |0\rangle$  gives the photon state with the amplitude at site  $m(n)$  described by  $v_{m(n)}(t)$ .  $H(t)$  is the time-dependent Hamiltonian of Eq. (1). The initial wave packet of the photon at  $t = 0$  has the form  $|\Psi(0)\rangle = \prod_{\eta=x,y,z} \exp[-(\eta - \eta_0)^2/w^2 + ik_\eta \eta]$ , where  $(x_0, y_0, z_0)$  is the center of wave packet with waist  $w$ . The results are plotted in Figure 3. In the absence of phase modulation, Figure 3(a) shows the initial wave packet of the photon. The wave packet propagates freely in the space with time and reaches to the corner of the lattice at  $t = 1.25 a/c$  (see Figure 3(b)). In contrast, in the presence of phase modulation with a choice of the amplitude  $\alpha = 2.40483$  and frequency  $\omega_M = 1.5 c/a$ , the wave packet of the photon is localized near its initial position throughout the entire duration of the simulation. This is demonstrated in Figs. 3(c) and (d), which show the wave packet's positions at  $t = 1.25 a/c$  and  $t = 5 a/c$ , respectively. The simulation here provides a direct visualization of the dynamic localization process in three dimensions.

Up to this point we have used the rotating wave approximation for the Hamiltonian in Eq. (1). Previous discussions on the photonic gauge field in this Hamiltonian have all assumed the rotating wave approximation. On the other hand, in the experimental demonstration of the photonic gauge field one often uses electro-optic modulation of refractive index [30]. In many electro-optic modulations, the strength of the modulation, as measured in  $\delta n/n \times \omega_0$ ,



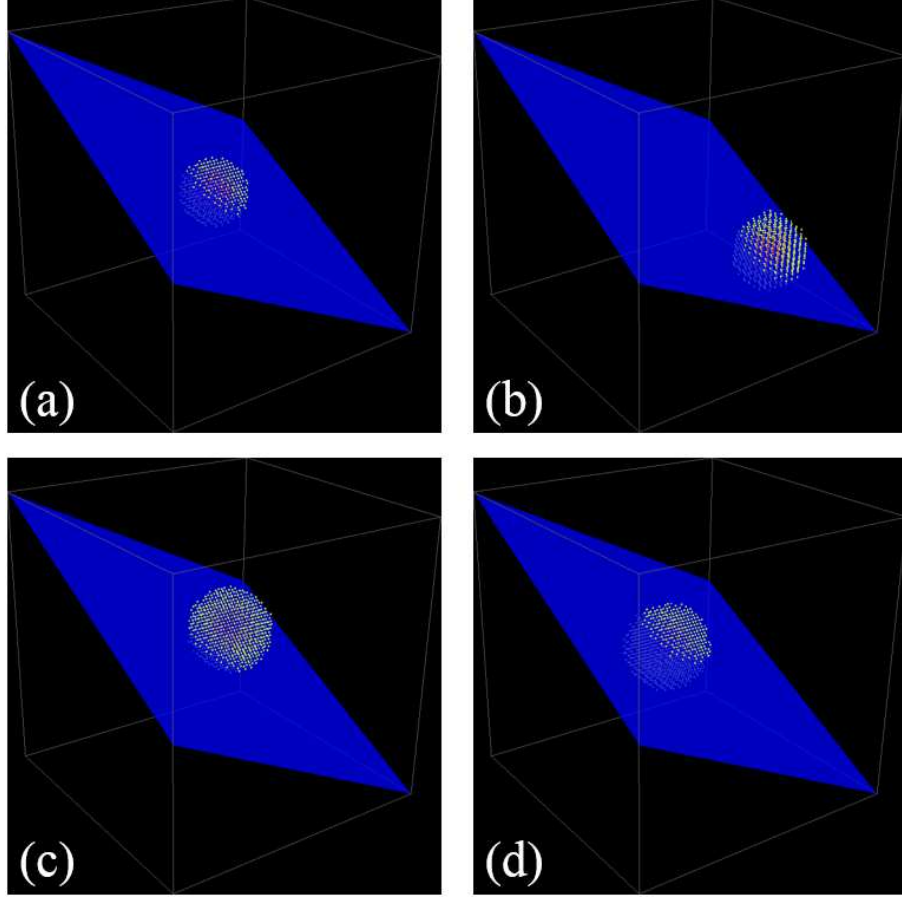


FIG. 3: (color online) Propagation of a photon wavepacket in a  $40a \times 40a \times 40a$  three dimensional lattice. (a) The initial condition at  $t = 0$ , with  $x_0 = y_0 = z_0 = 20 a$  and  $k_x = -k_y = -k_z = -1.283 a^{-1}$ ; (b) The wave packet at  $t = 1.25 a/c$  with no phase modulation; (c) and (d) The wave packet at  $t = 1.25 a/c$  and  $t = 5 a/c$ , respectively, with phase modulation. The parameters of the phase modulation are  $\alpha = 2.40483$  and  $\omega_M = 1.5 c/a$ . The coupling strength between the resonators is  $V = 2.4\pi c/a$ .

where  $n$  is the refractive index of the structure,  $\delta n$  is the index change, and  $\omega_0$  is the operating frequency, can be much larger than the modulation frequency  $\Omega$  on the order of a few GHz, therefore it is of importance to understand the validity of gauge potential concept beyond the rotating wave approximation. Here we show that the dynamic localization effect persists even in the regime where the rotating wave approximation is not valid.

We provide the results in one-dimension. The generalization to three-dimension is straightforward. For the treatment beyond the rotating wave approximation, we again starts by providing an intuitive treatment based on the instantaneous band-structure, we

then confirm the intuitive treatment through an exact numerical analysis of the Floquet bandstructure. The Hamiltonian (1) can be written in  $\mathbf{k}$ -space as:

$$H = \sum_{k_x} \left( \omega_A a_{k_x}^\dagger a_{k_x} + \omega_B b_{k_x}^\dagger b_{k_x} \right) + \sum_{k_x} V a_{k_x}^\dagger b_{k_x} \times (e^{i\Omega t} \cos[k_x a + \phi_x(t)] + e^{-i\Omega t} \cos[k_x a - \phi_x(t)]) + h.c.. \quad (11)$$

Perform the transformation  $c_{k_x} = e^{i\omega_{A(B)}t} a_{k_x} (b_{k_x})$ , we obtain

$$H = \sum_{k_x} V c_{k_x}^\dagger c_{k_x} \{ \cos[k_x a - \phi_x(t)] + \cos(2\Omega t) \cos[k_x a + \phi_x(t)] \}. \quad (12)$$

We notice that the first term is the same as Eq. (4) and the second term is the counter-rotating term. From Eq. (12) we can straightforwardly obtain the instantaneous bandstructure and hence the instantaneous group velocity at a wavevector  $k_x$ , since the Hamiltonian in the presence of counter rotating term is still periodic in real space. Again, assuming that the modulation phase  $\phi_x = \alpha \cos(\omega_M t)$ . The average group velocity over one phase modulation period ( $2\pi/\omega_M$ ) is

$$\langle v_g(k_x) \rangle = -V a \sin(k_x a) J_0(\alpha) - V a \frac{\omega_M}{2\pi} \int_0^{2\pi/\omega_M} dt \cos(2\Omega t) \sin[k_x a - \alpha \cos(\omega_M t)]. \quad (13)$$

To facilitate analytic calculation, we assume that

$$2\Omega = n\omega_M, \quad (14)$$

where  $n$  is a positive integer, the second term in Eq. (13), denoted as  $\langle v_g(k_x) \rangle_{\text{CR}}$ , can be calculated analytically as

$$\langle v_g(k_x) \rangle_{\text{CR}} = V a \times \begin{cases} (-1)^{m+1} \sin(k_x a) J_n(\alpha) & n = 2m \\ (-1)^m \cos(k_x a) J_n(\alpha) & n = 2m + 1 \end{cases}. \quad (15)$$

By choosing  $\alpha = 2.40483$ , which corresponds to  $J_0(\alpha) = 0$ , the first term in Eq. (13) vanishes. And the correction due to the second term can be made arbitrarily small by choosing a sufficiently large  $n$  in Eq. (14), i.e. by choosing the phase modulation frequency to be sufficiently small as compared to the frequency of coupling strength modulation. Thus, dynamic localization can still be accomplished in the regime where rotating wave approximation no longer applies. This result can be straightforwardly generalized to three-dimension. Three-dimensional dynamic localization should occur, when  $2\Omega = n\omega_M$ , provided that all bonds

along each direction has the same phase  $\phi_{x,y,z}(t) = \alpha \cos(\omega_M t)$  with the phase modulation amplitude  $\alpha$  being a zero's of  $J_0$ .

We confirm the intuitive analysis above by calculating the Floquet bandstructure in the case where  $V = 0.2\Omega$ , and hence the rotating wave approximation is no longer valid (blue lines in Figure 4), and by comparing such calculations to the prediction of the range of quasi-energies with rotating wave approximation. (Red lines in Figure 4). Figure 4(a) shows the case with  $\Omega = 2\omega_M$ . Introducing the counter rotating term indeed modifies the bandstructure. Nevertheless, the bandwidth still collapses near a phase modulation strength of  $\alpha = 2.40483$ . Thus, dynamic localization still occurs in this system beyond the rotating wave approximation. Figure 4(b) shows the case with  $\Omega = 4\omega_M$ . Comparing Figures 4(a) and 4(b), we observe that the discrepancy in the bandstructures between the cases with or without rotating wave approximation becomes smaller as  $\omega_M$  is reduced, in spite of the fact that with  $V = 0.2\Omega$  we are significantly outside the regime where the rotating wave approximation is valid. This observation is consistent with the analytic results derived above based on instantaneous bandstructure.

Experimentally, effective gauge field for photons have already been experimentally observed using two modulators [30]. The demonstration of the theoretical proposal here requires further integration of larger numbers of modulators. The experimental feasibility of such integration has been discussed in Ref. [32]. While for illustration purpose we have focused on a photonic gauge potential through the use of temporal refractive index modulation, the concept here should be relevant for other proposals of photonic gauge potential as well, include those based on magneto-optical effects [47, 48], as well as spin-dependent photonic gauge potential [49–53] and optomechanical gauge potential [54, 55]. In summary, we have shown that three-dimensional dynamic localization of light can be achieved with an effective gauge potential for photons. The results provide additional evidence of the exciting prospects of photonic gauge potential for the control of light propagation.

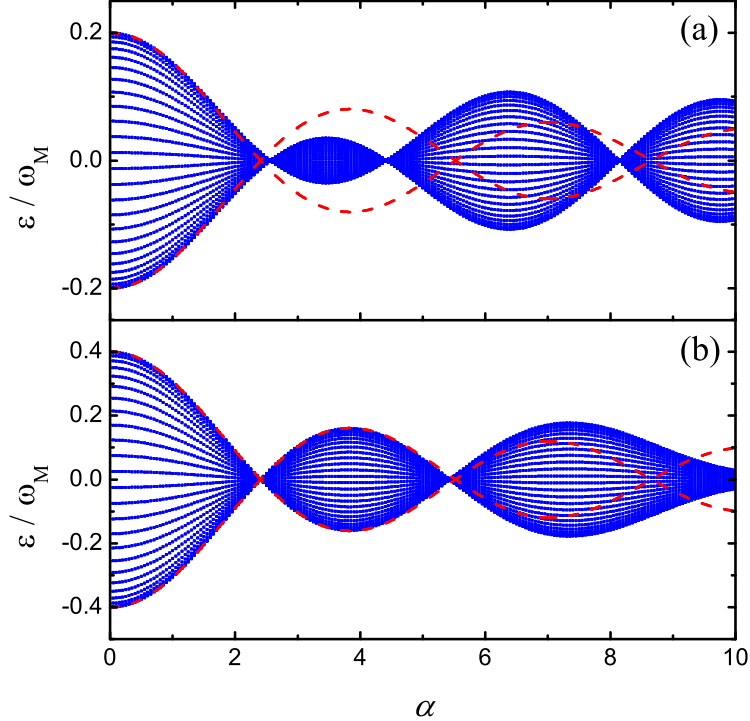


FIG. 4: (color online) Quasi-energies as a function of phase-modulation strength  $\alpha$ , for the Hamiltonian of Eq. (12), with  $\phi_x(t) = \alpha \cos(\omega_M t)$ .  $V = 0.2\Omega$ . (a)  $\Omega = 2\omega_M$ . (b)  $\Omega = 4\omega_M$ . Each blue curve corresponds to a different wavevector  $k_x$ , in the range of  $-\pi/a < k_x < \pi/a$ . Dashed red line is the envelope for the same Hamiltonian, but calculated using the rotating wave approximation.

### Acknowledgments

This work is supported in part by U.S. Air Force Office of Scientific Research Grant No. FA9550-09-1-0704 and U.S. National Science Foundation Grant No. ECCS- 1201914.

- 
- [1] D. H. Dunlap and V. M. Kenkre, *Phys. Rev. B* **34**, 3625 (1986).
  - [2] M. Holthaus, *Phys. Rev. Lett.* **69**, 351 (1992).
  - [3] G. Platero and R. Aguado, *Phys. Rep* **395**, 1 (2004).
  - [4] H. N. Nazareno and Y. Lépine, *Phys. Rev. B(R)* **55**, 6661 (1997).
  - [5] M. M. Dignam and C. Martijn de Sterke, *Phys. Rev. Lett.* **88**, 046806 (2002).
  - [6] Z. Wang, D. Suqing, and X. Zhao, *Phys. Rev. B* **69**, 035305 (2004).
  - [7] J. R. Madureira and P. A. Schulz, *Phys. Rev. B* **70**, 033309 (2004).

- [8] A. Eckardt, C. Weiss, and M. Holthaus, *Phys. Rev. Lett.* **95**, 260404 (2005).
- [9] C. E. Creffield and G. Platero, *Phys. Rev. Lett.* **105**, 086804 (2010).
- [10] N. Tsuji, T. Oka, P. Werner, and H. Aoki, *Phys. Rev. Lett.* **106**, 236401 (2011).
- [11] N. Singh, *Phys. Lett. A* **376**, 1593 (2012).
- [12] S. Longhi, *J. Phys.: Condens. Matter* **24**, 435601 (2012).
- [13] E. N. Bulgakov and A. R. Kolovsky, *Phys. Rev. B* **89**, 035116 (2014).
- [14] K. W. Madison, M. C. Fischer, R. B. Diener, Q. Niu, and M. G. Raizen, *Phys. Rev. Lett.* **81**, 5093 (1998).
- [15] A. Eckardt, M. Holthaus, H. Lignier, A. Zenesini, D. Ciampini, O. Morsch, and E. Arimondo, *Phys. Rev. A* **79**, 013611 (2009).
- [16] S. John, *Phys. Rev. Lett.* **58**, 2486 (1987).
- [17] I. L. Garanovich, S. Longhi, A. A. Sukhorukov, and Y. S. Kivshar, *Phys. Rep* **518**, 79 (2012).
- [18] P. W. Anderson, *Phys. Rev.* **109** 1492 (1958).
- [19] T. Schwartz, G. Bartal, S. Fishman, and M. Segev, *Nature* **446**, 52 (2007).
- [20] Y. Lahini, A. Avidan, F. Pozzi, M. Sorel, R. Morandotti, D. N. Christodoulides, and Y. Silberberg, *Phys. Rev. Lett.* **100**, 013906 (2008).
- [21] M. Segev, Y. Silberberg, and D. N. Christodoulides, *Nat. Photonics* **7**, 197 (2013).
- [22] S. Longhi, *Opt. Lett.* **30**, 2137 (2005).
- [23] S. Longhi, M. Marangoni, M. Lobino, R. Ramponi, and P. Laporta, *Phys. Rev. Lett.* **96**, 243901 (2006).
- [24] A. Szameit, I. L. Garanovich, M. Heinrich, A. A. Sukhorukov, F. Dreisow, T. Pertsch, S. Nolte, A. Tünnermann, and Y. S. Kivshar, *Nat. Phys.* **5**, 271 (2009).
- [25] A. Szameit, I. L. Garanovich, M. Heinrich, A. A. Sukhorukov, F. Dreisow, T. Pertsch, S. Nolte, A. Tünnermann, S. Longhi, and Y. S. Kivshar, *Phys. Rev. Lett.* **104**, 223903 (2010).
- [26] A. Joushaghani, R. Iyer, J. K. S. Poon, and J. W. Aitchison, *Phys. Rev. Lett.* **109**, 103901 (2012).
- [27] A. Crespi, G. Corrielli, G. D. Valle, R. Osellame, and S. Longhi, *New J. Phys.* **15**, 013012 (2013).
- [28] K. Fang, Z. Yu, and S. Fan, *Phys. Rev. Lett.* **108**, 153901 (2012).
- [29] K. Fang, Z. Yu, and S. Fan, *Phys. Rev. B(R)* **87**, 060301 (2013).
- [30] L. D. Tzuang, K. Fang, P. Nussenzeig, S. Fan, and M. Lipson, *Nat. Photonics* **8**, 701 (2014).

- [31] E. Li, B. J. Eggleton, K. Fang, and S. Fan, *Nat. Commun.* **5**, 3225 (2014).
- [32] K. Fang, Z. Yu, and S. Fan, *Nat. Photonics* **6**, 782 (2012).
- [33] K. Fang and S. Fan, *Phys. Rev. Lett.* **111**, 203901 (2013).
- [34] K. Fang, Z. Yu, and S. Fan, *Opt. Express* **21**, 18216 (2013).
- [35] Q. Lin and S. Fan, *Phys. Rev. X* **4**, 031031 (2014).
- [36] See Supplemental Material [url], which includes Refs. [32, 37–40].
- [37] J. N. Winn, S. Fan, J. D. Joannopoulos, and E. P. Ippen, *Phys. Rev. B* **59**, 1551 (1999).
- [38] M. P. C. Taverne, Y. D. Ho, and J. G. Rarity, *J. Opt. Soc. Am. B* **32**, 639 (2015).
- [39] M. Qi, E. Lidorikis, P. T. Rakich, S. G. Johnson, J. D. Joannopoulos, E. P. Ippen, and H. I. Smith, *Nature* **429**, 538 (2004).
- [40] L. A. Woldering, A. P. Mosk, and W. L. Vos, *Phys. Rev. B* **90**, 115140 (2014).
- [41] M. Reichelt and T. Meier, *Opt. Lett.* **34**, 2900 (2009).
- [42] J. Ma, L. J. Martinez, S. Fan, and M. L. Povinelli, *Opt. Express* **21**, 2463 (2013).
- [43] R. Novitski, B. Z. Steinberg, and J. Scheuer, *Opt. Express* **22**, 23153 (2014).
- [44] M. Bayindir, B. Temelkuran, and E. Ozbay, *Phys. Rev. Lett.* **84**, 2140 (2000).
- [45] J. H. Shirley, *Phys. Rev.* **138**, B979 (1965).
- [46] H. Samba, *Phys. Rev. A* **7**, 2203 (1973).
- [47] R. O. Umucalilar and I. Carusotto, *Phys. Rev. A* **84**, 043804 (2011).
- [48] K. Fang and S. Fan, *Phys. Rev. A* **88**, 043847 (2013).
- [49] M. Hafezi, E. A. Demler, M. D. Lukin, and J. M. Taylor, *Nat. Phys.* **7**, 907 (2011).
- [50] M. Hafezi, S. Mittal, J. Fan, A. Migdall, and J. M. Taylor, *Nat. Photonics* **7**, 1001 (2013).
- [51] A. B. Khanikaev, S. H. Mousavi, W. -K. Tse, M. Kargarian, A. H. MacDonald, and G. Shvets, *Nature Materials* **12**, 233 (2013).
- [52] M. C. Rechstman, J. M. Zeuner, Y. Plotnik, Y. Lumer, D. Podolsky, F. Dreisow, S. Nolte, M. Segev, and A. Szameit, *Nature* **496**, 196 (2013).
- [53] S. Mittal, J. Fan, A. Faez, J. M. Taylor, and M. Hafezi, *Phys. Rev. Lett.* **113**, 087403 (2014).
- [54] M. Schmidt, V. Peano, and F. Marquardt, arXiv:1131.7095v2.
- [55] V. Peano, C. Brendel, M. Schmidt, and F. Marquardt, arXiv:1409.5375v1.